Available online at www.sciencedirect.com
ScienceDirect
Trans. Nonferrous Met. Soc. China 21(2011) 2408−2414
Transactions of Nonferrous Metals Society of China
www.tnmsc.cn

Microstructure and mechanical properties of Fe_3Al alloys prepared by MA-PAS and MA-HP

WANG Jian[1], XING Jian-dong[2], TANG Hui-ping[1], YANG Bao-jun[1], LI Ya-ning[1]

1. State Key Laboratory of Porous Metal Materials, Northwest Institute for Nonferrous Metal Research, Xi'an 710016, China;
2. State Key Laboratory for Mechanical Behavior of Materials, Xi'an Jiaotong University, Xi'an 710049, China

Received 30 June 2011; accepted 30 September 2011

Abstract: Fe_3Al alloys with nearly full density were fabricated by plasma activated sintering (PAS) and hot pressing (HP) from mechanical alloyed Fe-28%Al (mole fraction) powders, respectively. It is found that A2-type Fe_3Al alloys were obtained by PAS, and they had a heterogeneous grain size distribution, most areas had a grain size smaller than 500 nm, and other areas had a grain size of about 1 μm. Different to PAS, $D0_3$-type Fe_3Al alloys with a grain size of of 1−2 μm were obtained by HP. The compression testing results show that yield strength values of Fe_3Al alloys fabricated by PAS and HP are almost equal at an elevated temperature, and the compression yield strength was about 100 MPa for all at 800 °C. The room temperature compression ductility of Fe_3Al alloys by PAS was about 20%, which was superior to that of Fe_3Al alloys prepared by HP and casting.

Key words: Fe_3Al intermetallic; plasma activated sintering; hot pressing; microstructure; mechanical properties

1 Introduction

Iron aluminides based on Fe_3Al alloys exhibit a combination of excellent oxidation and sulfidation resistance, low materials cost and compared strength favorably with many ferritic and austenitic stainless steels, which makes them very attractive as candidate materials for high temperature applications. However, limited ductility at room temperature and a sharply drop in strength above 600 °C have been major deterrents to their acceptance for many structural applications [1−4].

In recent years, several attempts have been made to improve their ductility and strength by means of grain refinement, which can be easily achieved by mechanical alloying (MA) technology. The fabrication of Fe_3Al powders by MA has been extensively studied by many groups, and all of these studies reported that disordered A2-type Fe_3Al alloys (Fe(Al) solid solution) with nano-sized grains tended to form Fe−Al powder mixtures [5−9]. In addition, several consolidation processes have been used to retain the ultrafine microstructure of the mechanical alloyed powders, such as hot pressing (HP) [10−13], hot isostatic pressing (HIP) [14] and plasma activated sintering (PAS) or spark plasma sintering (SPS) [15−22]. Among them, PAS and SPS have advantages of short sintering time and low sintering temperature, and have been proved to be very potent to retain the ultrafine microstructure of the original milled powders to produce bulk nanostructured materials. On the other hand, disordered A2-type Fe_3Al, which is the metastable phase at room temperature according to the equilibrium phase diagram of Fe−Al, will transfer to ordered B2 or $D0_3$ phase after sintering in theory. Therefore, it is necessary to study the effect of consolidation processing on grain size and ordering structure of Fe_3Al alloys, which exert a large influence on their mechanical properties.

In this work, nanocrystalline powders were firstly fabricated by MA, and subsequently the mechanical alloyed powders were consolidated by two different processes, PAS and HP, respectively. The microstructure and compression properties of as-sintered Fe_3Al alloys were studied in detail.

2 Experimental

Pure elemental iron powder and aluminum powders (particle size smaller than 75 μm) were blended in the

Foundation item: Project (50871084) supported by the National Natural Science Foundation of China; Project (2009AA032601) supported by the National High Technology Research and Development Program of China
Corresponding author: WANG Jian; Tel: +86-29-86231095; E-mail: jwangxjtu@163.com
DOI: 10.1016/S1003-6326(11)61028-5

mole ratio of 72:28 to produce the pre-alloyed powders by MA. MA was carried out at room temperature for up to 50 h in a XQM−4L planetary ball mill operating at 250 r/min. The ball to powder mass ratio was maintained at 10:1 throughout the investigation. To minimize oxidation of the powder mixture, the steel vial was first evacuated with a vacuum pump, and then filled with argon with a purity of 99.99%. In addition, 0.5 mL methanol was used as process control agent to avoid cold welding during MA.

The mechanically alloyed powders were sieved to particle size smaller than 75 μm, and consolidated by PAS and HP, respectively. An Ed-PASIII apparatus was used for the PAS processing. At the beginning of the PAS process, a pulsed voltage potential was used, and then the powders were heated up at the rate of 2 °C/s by resistance heating. Consolidation was performed at a selected sintering temperature of 1 000 °C for a holding time of 180 s. The cooling rate was about 1 °C/s. A uniaxial load of 30 MPa was applied during the whole heating and cooling stages. The whole time used for PAS was about 30 min. The HP process was carried out under a pressure of 30 MPa using a universal HP apparatus with a vacuum of 1.33×10^{-2} Pa in its chamber. The powders were heated up at the rate of 15 °C/min, and consolidated at 1 200 °C for 30 min，and then slowly cooled in the furnace. The whole time used for HP was about 10 h. The relative density of the consolidated compacts was measured by the Archimedes immersion technique with deionized water.

Phase analyses of mechanical alloyed powders and sintered compacts were carried out by X-ray diffraction (XRD) using RIGAKU D/MAX−2400 diffractometer with a Cu-target. Average grain size of the mechanical alloyed powders was determined from the line broadening of the (110) fundamental line of the alloys using Scherrer formula [23] and by incorporating instrumental broadening which was determined by recording calibration spectra of pure Fe powders. Microstructure of consolidated compacts was characterized using a scanning electron microscope (SEM). A JEM−200CX transmission electron microscope (TEM) was used to determine the ordering state and grain size of consolidated compacts.

Cylindrical compression samples with 4 mm in diameter and 6 mm in height were machined along the long axis parallel to the pressing direction. The compression tests were carried out from room temperature to 800 °C in air using a Gleeble 1500D testing system at a strain rate of 2×10^{-3} s^{-1}. To minimize the friction effect, the specimen-die interface was lubricated with silicon carbides.

3 Results

Figure 1 shows the typical X-ray diffraction patterns of the mixed powders before and after milling. The diffraction patterns show the formation of A2-type Fe_3Al alloys after milling for 50 h. The average grain size of the as-milled powders estimated from the line width of the fundamental (110) line using Scherrer formula was about 12 nm.

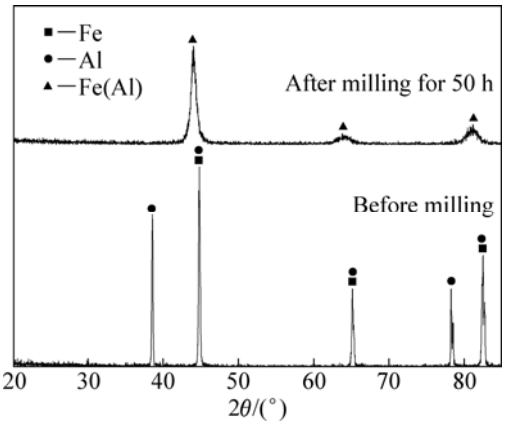

Fig. 1 XRD patterns of mixed powders before and after milling

Figure 2 shows the SEM (BSE mode) micrographs of polished compacts by PAS and HP, respectively. It can be seen that there are fewer pores in compacts by PAS, which evidences good quality of consolidation. The measured relative densities of the compacts were 99.8% and 98.1%, respectively, for PAS and HP.

Figure 3 shows the typical X-ray diffraction patterns

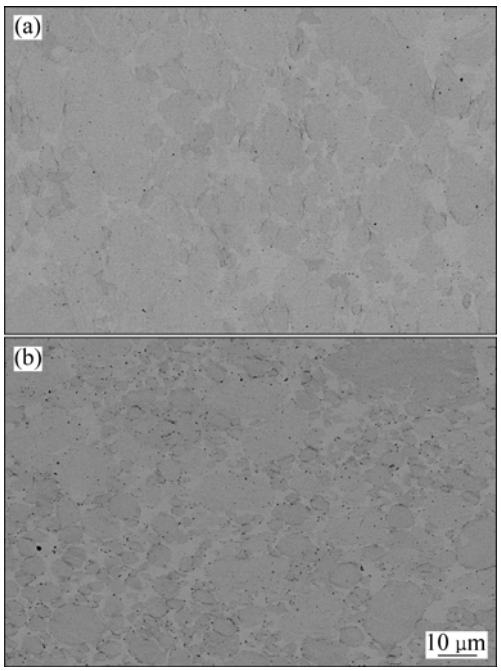

Fig. 2 SEM images of polished compacts by PAS (a) and HP (b)

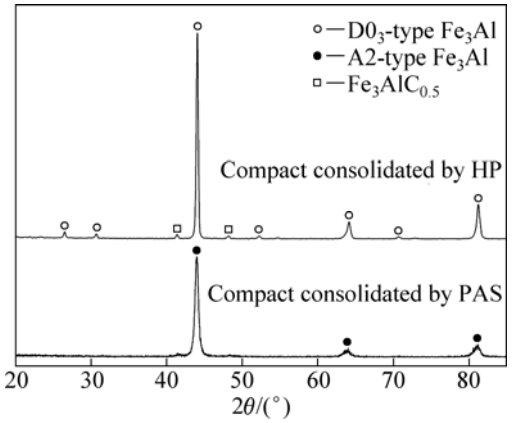

Fig. 3 XRD patterns of Fe_3Al by HP and PAS

of the compacts by PAS and HP, respectively. It can be seen that the XRD pattern of compacts by PAS is similar to that of milled powders, and none superlattice reflections of ordered B2-type or $D0_3$-type Fe_3Al was observed for compacts by PAS. So, it can preliminarily deduce that disorder−order transformation did not occur during PAS. However, different from PAS, ordered $D0_3$-type superlattice reflections are obviously observed for compacts by HP, and it evidences the ordering of Fe_3Al alloys occurring during HP. In addition, the ordering degree S can be evaluated by measuring the intensity of the superlattice reflections relative to that of the fundamental reflections according to Eq. (1) [23]:

$$S=\sqrt{\frac{I_{S(dis)}/I_{F(dis)}}{I_{S(ord)}/I_{F(ord)}}} \tag{1}$$

where I_S and I_F represent the integrated intensities of the superlattice and fundamental reflection, respectively; the subscripts (dis) and (ord) refer to the disordered and ordered states, respectively. PDF 65−3006 card was used to calculate the ordering degree, and the calculated ordering degree is 0.69 by Eq. (1). Another feature in the XRD patterns is that the peaks of $Fe_3AlC_{0.5}$ are observed in all compacts. The precipitation of $Fe_3AlC_{0.5}$ is due to the contamination from methanol during milling, which has been proved by many other researchers [15, 18].

TEM investigations were performed in order to evaluate the grain size and further study ordering state of the consolidated compacts. Figure 4 shows the typical TEM images of compacts by PAS. It can be seen that the compacts by PAS show a heterogeneous grain size distribution, most areas had a grain size smaller than 500 nm, and other areas had a grain size of about 1 μm. In addition, selected area diffraction patterns further reveal that disordered phase was obtained by PAS.

Figure 5(a) shows the TEM image of compacts consolidated by HP. It can be seen that the grain size of the compacts consolidated by HP is 1−2 μm, and the

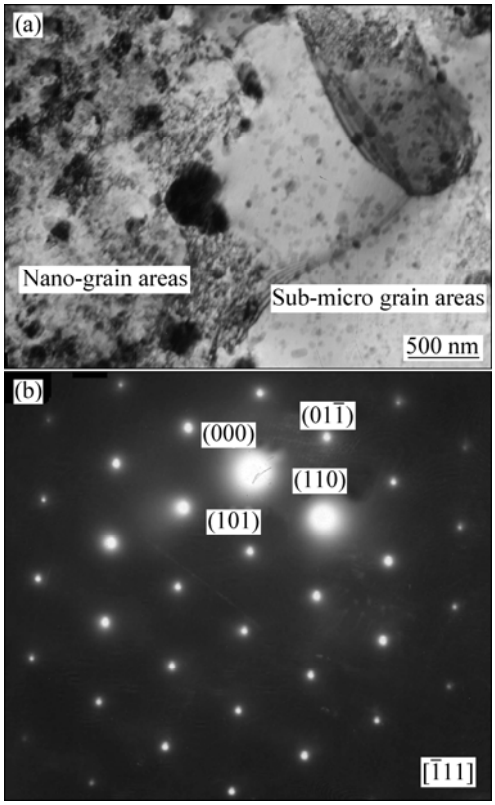

Fig. 4 Bright-field transmission micrograph of Fe_3Al by PAS (a) and electron diffraction pattern (b)

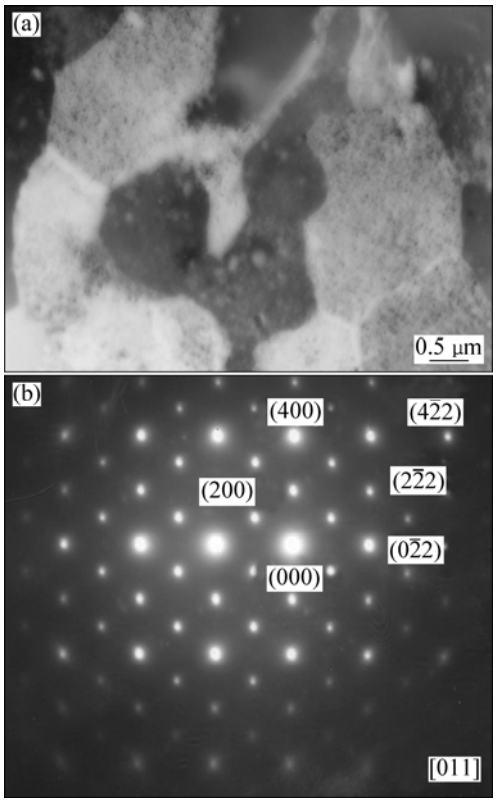

Fig. 5 Bright-field transmission micrograph of Fe_3Al by HP (a) and electron diffraction pattern (b)

selected area diffraction pattern (Fig. 5(b)) further reveals that ordered $D0_3$ phase was obtained by HP.

Figure 6 shows the engineering stress — strain curves for the consolidated compacts tested at room temperature in compression. It can be seen that compacts by PAS exhibit more superior rupture strain than compacts by HP, the rupture strain values of consolidated compacts are 14% and 20%, respectively, for PAS and HP. Compared with 12% of as-cast Fe_3Al alloys [24], the value of compacts by PAS is more superior. Temperature dependence of the yield strength of consolidated compacts is shown in Fig. 7. It can be seen that the yield strength values of Fe_3Al alloys fabricated by PAS and HP are almost equal at an elevated temperature. Although the yield strength drops sharply above 400 °C, which is similar to the as-cast Fe_3Al alloy, the compression yield strength is about 100 MPa for all the same at 800 °C, and it is much higher than that of as-cast Fe_3Al alloys [24].

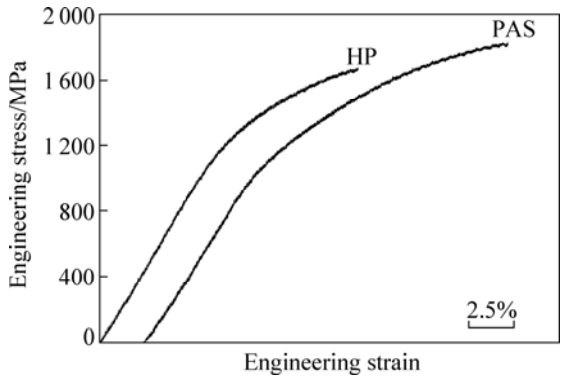

Fig. 6 Room temperature compression engineering stress—strain curves of Fe_3Al alloys by HP and PAS

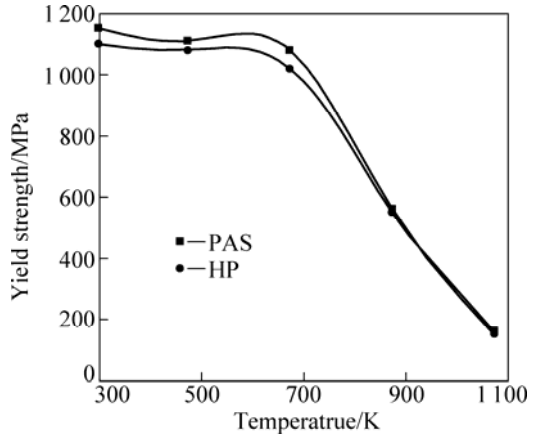

Fig. 7 Temperature dependence of compression yield strength of Fe_3Al alloys by PAS and HP

4 Discussion

4.1 Disorder-order transformation during consolidation

It is well known that the disorder-order transformation during consolidation is driven by the energy difference between ordered and disordered states (ordering energy), and affected by the consolidation and cooling process. Formation enthalpy of disordered and ordered intermetallic compound formed from a mixture of pure elements A and B can be calculated by the Miedema's semi-empirical model.

According to Miedema model, the formation enthalpy of disordered and ordered Fe_3Al can be obtained according to Eq. (2) [25−26].

$$\Delta H = \Delta H_C + \Delta H_E + \Delta H_S \tag{2}$$

where ΔH_C, ΔH_E and ΔH_S are the chemical, elastic and structural contribution due to mixing atoms, size mismatch and the difference in valence electrons and crystal structure of solute and solvent atoms, respectively.

ΔH_C can be calculated using Eq. (3).

$$\Delta H_C = \frac{2Pf(c)(c_A v_A^{2/3} + c_B v_B^{2/3})}{(n_{ws}^A)^{-1/3} + (n_{ws}^B)^{-1/3}} \times \left[-(\Delta \Phi^*)^2 + \frac{Q}{P}(\Delta n_{ws}^{1/3})^2 - \frac{R'}{P} \right] \tag{3}$$

where c_A and c_B are the mole fractions of elements A and B, respectively; Φ^*, v and n_{ws} are work functions, molar volume and electron density of the constituents, respectively; P, Q and R' are empirical constants. For binary alloys between the transitional and non-transitional elements, P=12.35 kJ/(V^2·cm), Q=116.09 kJ/V and R'/P=1.9; $f(c)$ is the concentration function, and the value of $f(c)$ for disordered and ordered Fe_3Al can be calculated by Eqs. (4) and (5), respectively. For disordered Fe_3Al:

$$f(c) = c_A^S c_B^S \tag{4}$$

For ordered Fe_3Al:

$$f(c) = c_A^S c_B^S [1 + 8(c_A^S c_B^S)^2] \tag{5}$$

where c_A^S and c_B^S are the surface concentration of elements A and B, respectively, and they can be calculated by Eqs. (6) and (7), respectively.

$$c_A^S = \frac{c_A v_A^{2/3}}{c_A v_A^{2/3} + c_B v_B^{2/3}} \tag{6}$$

$$c_B^S = \frac{c_B v_B^{2/3}}{c_A v_A^{2/3} + c_B v_B^{2/3}} \tag{7}$$

ΔH_E, the elastic contribution of enthalpy, can be calculated by Eq. (8) [27].

$$\Delta H_E = c_A c_B (c_A \Delta E_{AinB} + c_B \Delta E_{BinA}) \tag{8}$$

where ΔE_{AinB} and ΔE_{BinA} are the elastic energies caused

by A dissolving in B and B dissolving in A, respectively, and they can be calculated by Eqs. (9) and (10), respectively.

$$\Delta E_{\mathrm{AinB}}=\frac{2K_{\mathrm{A}}\mu_{\mathrm{B}}(v_{\mathrm{B}}-v_{\mathrm{A}})^2}{3K_{\mathrm{A}}v_{\mathrm{B}}+4\mu_{\mathrm{B}}v_{\mathrm{A}}} \tag{9}$$

$$\Delta E_{\mathrm{BinA}}=\frac{2K_{\mathrm{B}}\mu_{\mathrm{A}}(v_{\mathrm{A}}-v_{\mathrm{B}})^2}{3K_{\mathrm{B}}v_{\mathrm{A}}+4\mu_{\mathrm{A}}v_{\mathrm{B}}} \tag{10}$$

where K and μ are bulk modulus and shear modulus, respectively.

For the binary alloys between the transitional and non-transitional elements [28], there is

$\Delta H_{\mathrm{S}}=0$

Parameters used in the Miedema model are shown in Table 1.

Table 1 Parameters of Miedema model [29−30]

Element	$n^{1/3}$/ cm^{-1}	v/ $(\mathrm{cm}^3\cdot\mathrm{mol}^{-1})$	Φ^*/V	K/ 10^4MPa	μ/ 10^4MPa
Fe	1.77	7.10	4.93	21.14	8.16
Al	1.39	4.64	4.20	7.52	2.62

The formation enthalpies of disordered and ordered Fe_3Al for Fe-28Al system calculated based on the Miedema model are −18.04 kJ/mol and −24.88 kJ/mol, respectively, and the difference (ordering energy) is only 6.84 kJ/mol.

Based on above calculation results, it can be seen that ordering energy of Fe_3Al is significantly lower, so its tendency to reordering is lower. In the present study, the cooling rate is relatively high during PAS, so the reordering almost has no time to occur and the disordered phase is mostly retained by PAS. In contrast, the cooling rate during HP is relatively low and ordered Fe_3Al alloys are mostly obtained by HP.

4.2 Grain growth during consolidation

It is well known that grain growth will occur during consolidation and cooling process. Due to relatively low consolidation temperature and high cooling rate, some areas with nano grain size were retained by PAS. In addition, at the beginning of the PAS process, necks connecting powder particles can be quickly formed with the aid of a pulsed direct current, and the temperature at the neck must be much higher than that in the rest of the powder particles due to a higher current density [31−32]. Such effect associated with the applied uniaxial pressure allows the grains of the neck to a fast growth. Therefore, a heterogeneous grain size distribution was observed in the compacts by PAS. In contrast, due to relatively high consolidation temperature and very slowly cooling rate, larger grains reaching a size of 1−2 μm were obtained by HP.

4.3 Mechanical properties of consolidated Fe_3Al

The mechanical properties of Fe_3Al are very sensitive to many factors including alloying addition, environment, order (type, amount, size of ordered domains), and grain size [4]. In the present study, the room temperature yield strengths of compacts consolidated by PAS and HP were both improved compared with as-cast Fe_3Al materials. The improvement of strength can be explained by the well known Hall-Petch relationship. By comparing the two consolidation methods, it can be found almost equal room temperature yield strength was obtained in compacts consolidated by two different methods, although the grain size of compacts consolidated by PAS is smaller than that consolidated by HP. However, different from disordered alloys, dislocation slip in ordered Fe_3Al can be inhibited not only by grain boundaries but by anti-phase domain boundaries, as shown in Fig. 8, which is beneficial to strengthening of materials. Therefore, Fe_3Al by HP has almost equal yield strength to disordered Fe_3Al alloys by PAS, although which has smaller grain size.

On the other hand, ductility of materials can also be improved by grain refinement for most disordered polycrystalline metallic materials. So, the improvement in ductility of disordered alloys by PAS can be explained by grain refinement mechanism. However, for ordered Fe_3Al by HP, although the grain size of consolidated compacts is also smaller than that of as-cast Fe_3Al alloys, only slight improvement in ductility was observed compared with coarse-grained as-cast Fe_3Al materials, and the similar phenomenon was found in Fe-45Al alloys by COHRON et al [33]. Furthermore, BAKER and MUNROE [34] concluded that the slight improvements in ductility by grain refinement were generally overshadowed or confused with environmental

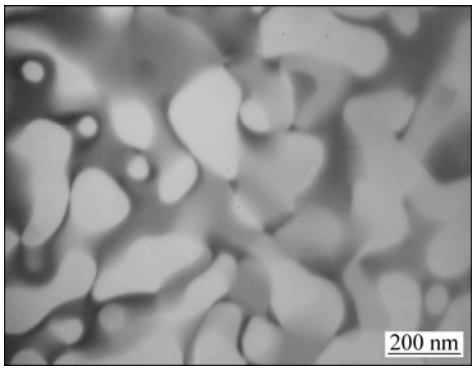

Fig. 8 Anti-phase domain of Fe_3Al by HP (dark field micrograph taken using [111] super reflections)

embrittlement effect, which involves hydrogen generated from the reaction of aluminum atoms in the alloys with water vapor in the air [35]. In addition, SU et al [36] studied the effect of atomic order on environmental embrittlement of Fe_3Al, and found that the ordered structure is much more susceptible to the test environments than the disordered structure. Based on above report and present study, it can be deduced that the improvement in room temperature ductility for Fe_3Al alloys by PAS is attributed to the combined effect of grain refinement and disordering.

5 Conclusions

1) Nanocrystalline Fe(Al) solid solution powders by mechanical alloying were consolidated by PAS and HP, respectively. The measured relative densities of the compacts were 99.8% and 98.1%, respectively, for PAS and HP.

2) A2-type Fe_3Al alloys were obtained by PAS, with a heterogeneous grain size distribution, and most areas had a grain size smaller than 500 nm, and other areas had a grain size of about 1 μm. However, $D0_3$-type Fe_3Al alloys with a grain size of 1−2 μm were obtained by HP.

3) Due to grain refinement, the compression yield strength of Fe_3Al alloys at elevated temperature was both improved by PAS and HP processes compared with as-cast alloy, although the strength also decreased sharply above 400 °C.

4) Obvious improvement in room temperature ductility was only observed in A2-type Fe_3Al alloys by PAS compared with as-cast Fe_3Al alloys, due to the disordering structure and much smaller grain size resulting from PAS processing.

References

[1] STOLOFF N S. Iron aluminides: Present status and future prospects [J]. Mater Sci Eng A, 1998, 258(1): 1−14.

[2] LIU C T, STRINGER J, MUNDY J N, HORTON L L, ANGELINI P. Ordered intermetallic alloys: An assessment [J]. Intermetallics, 1997, 5(8): 579−596.

[3] STOLOFF N S, LIU C T, DEEVI S C. Emerging application of intermetallics [J]. Intermetallics, 2000, 8(9−11): 1313−1320.

[4] DEEVI S C, SIKKA V K, LIU C T. Processing, properties, and application of nickel and iron aluminides [J]. Prog Mater Sci, 1997, 42(1−4): 177−192.

[5] SURYANARAYANA C. Mechanical alloying and milling [J]. Prog Mater Sci, 2001, 469(1−2): 1−184.

[6] FAIR G H, WOOD J V. Mechanical alloying of iron-aluminium intermetallics [J]. Powder Metallurgy, 1993, 36(2): 123−128.

[7] FAN Run-hua, SUN Jia-tao, GONG Hong-yu, SUN Kang-ning, WANG Wei-min. Structural evolution of mechanical alloyed nanocrystalline Fe-28Al powders [J]. Powder Technol, 2005, 149(2−3): 121−126.

[8] TANG W M, ZHENG Z X, TANG H J, REN R, WU Y C. Structure evolution and grain growth kinetic of the Fe-28Al elemental powder during mechanical alloying and annealing [J]. Intermetallics, 2007, 15(8): 1020−2026.

[9] ENZO S, FRATTINI R, GUPTA R, MACRI P P, PRINCIPI G, SCHIFFIN L, SCIPIONE G. X-ray powder diffraction and Mossbauer study of nanocrystalline Fe-Al prepared by mechanical alloying [J]. Acta Mater, 1996, 44(8): 3105−3113.

[10] KRASNOWSKI M, KULIK T. Nanocrystalline FeAl intermetallic produced by mechanical alloying followed by hot-pressing consolidation [J]. Intermetallics, 2007,15(2): 201−205.

[11] KRASNOWSKI M, KULIK T. Nanocrystalline FeAl matrix composites reinforced with TiC obtained by hot-pressing consolidation of mechanically alloyed powders [J]. Intermetallics, 2007, 15(10): 1377−1383.

[12] HE L, MA E. Nanophase metallic alloys consolidated from powders prepared by mechanical alloying [J]. Mater Sci Eng A,1995, 204(1): 240−245.

[13] MORRIS-MUÑOZ M A, DODGE A, MORRIS D G. Structure, strength and toughness of nanocrystalline FeAl [J]. Nanostruct Mater, 1999, 11(7): 873−885.

[14] ZHU Su-ming, TAMURA M, SAKAMOTO K, IWASAKI K. Characterization of Fe_3Al-based intermetallic alloys fabricated by mechanical alloying and HIP consolidation [J]. Mater Sci Eng A, 2000, 292(1): 83−89.

[15] ZADRA M, CASARI F, LONARDELLI I, ISCHIA G, MOLINARI A. In-situ precipitation of Al_2O_3 and K-$Fe_3AlC_{0.5}$ in iron aluminides through spark plasma sintering: Microstructure and mechanical properties [J]. Intermetallics, 2007, 15(12): 1650−1658.

[16] VENKATASWAMY M A, SCHNEIDER J A, GROZA J R, MUKHERJEE A K, YAMAZAKI K, SHOOA K. Mechanical alloying processing and rapid plasma activated sintering consolidation of nanocrystalline iron-aluminides [J]. Mater Sci Eng A , 1996, 207(2): 153−158.

[17] PARK B G, KO S H, PARK Y H, LEE J H. Mechanical properties of in situ Fe_3Al matrix composites fabricated by MA–PDS process [J]. Intermetallics, 2006, 14(6): 660−665.

[18] MINAMINO Y, KOIZUMI Y, TSUJI N, HIROHATA N, MIZUUCHI K, OHKANDA Y. Microstructure and mechanical properties of bulk nanocrystalline Fe-Al-C alloys made by mechanically alloying with subsequent spark plasma sintering [J]. Sci Technol Adv Mater, 2004, 5(1−2): 133−143.

[19] HE Qing, JIA Cheng-chang, MENG Jie. Influence of iron powder particle size on the microstructure and properties of Fe_3Al intermetallics prepared by mechanical alloying and spark plasma sintering [J]. Mater Sci Eng A, 2006, 428(1−2): 314−318.

[20] SASAKI T T, OHKUBO T, HONO K. Microstructure and mechanical properties of bulk nanocrystalline Al-Fe alloy processed by mechanical alloying and spark plasma sintering [J]. Acta Mater, 2009, 57(12): 3529−3538.

[21] PARIS S, GAFFET E, BERNARD F, MUNIR Z A. Spark plasma synthesis from mechanical activated powders: A versatile route for producing dense nanostructured iron aluminides [J]. Scr Mater, 2004, 50(5): 691−696.

[22] JI Gang, GROSDIDIER T, BOZZOLO N, LAUNOIS S. The mechanisms of microstructure formation in a nanostructured oxide dispersion strengthened FeAl alloy obtained by spark plasma sintering [J]. Intermetallics, 2007, 15(2): 108−118.

[23] SURYANARAYANA C, NORTON M G. X-ray diffraction: A practical approach [M]. New York: Plenum, 1998.

[24] FALAT L, SCHNEIDER A, SAUTHOFF G, FROMMEYER G. Mechanical properties of Fe-Al-M-C (M=Ti, V, Nb, Ta) alloys with strengthening carbides and Laves phase [J]. Intermetallics, 2005, 13(12): 1256−1262.

[25] MIEDEMA A R, de CHÂTEL P F, de BOER F R. Cohesion in alloys-fundamental of a semi-empirical model [J]. Physica B, 1980,

100(1): 1−28.
[26] MIEDEMA A R, de BOER F R, BOOM R. Predicting heat effects in alloys [J]. Physica B, 1981, 103(1): 67−81.
[27] NIESSEN A K, MIEDEMA A R. The enthalpy effect on forming diluted solid solution of two 4d and 5d transition metals [J]. Bunsenges Ber Phys Chem, 1983, 87(9): 717−725.
[28] LÓPEZ J M, ALONSO J A, GALLEGO L J. Determination of the glass-forming concentration range in binary alloys from a semiempirical theory: Application to Zr-based alloys [J]. Phys Rev B, 1987, 36(7): 3716−3722.
[29] de BOER F R, BOOM R, MATTENS W C, MIEDEMA A R, NIESSEN A K. Cohesion in metal: Transition metal alloys [M]. Amsterdam, North-Holland, 1988.
[30] YAN Wei-lin, FANG Liang, SUN Kun, XU Yun-hua. Thermodynamics of nanocrystalline formation in surface layer of Hadfield steel by shot peening [J]. Mater Sci Eng A, 2007, 445−446: 392−397.
[31] ORRÙ R, LICHERI R, LOCCI A M, CINCOTTI A, GIACOMO C. Consolidation/synthesis of materials by electric current activated/assisted sintering [J]. Mater Sci Eng R, 2009, 63(4−6): 127−287.
[32] SONG Xiao-yan, LIU Xue-mei, ZHANG Jiu-xing. Neck formation and self-adjusting mechanism of neck growth of conducting powders in spark plasma sintering [J]. J Am Ceram Soc, 2006, 89(2): 494−500.
[33] COHRON J W, LIN Y, ZEE R H, GEORGE E P. Room-temperature mechanical behavior of FeAl: Effect of stoichiometry environment and boron addition [J]. Acta Mater, 1998, 46(17): 6245−6256.
[34] BAKER I, MUNROE P R. Mechanical properties of FeAl [J]. Int Mater Rev, 1997, 42(5): 181−205.
[35] LIU C T, MCKAMEY C G, LEE E H. Environmental effects on room-temperature ductility and fracture in Fe_3Al [J]. Scr Mater, 1990, 24(2): 385−389.
[36] SU Jiang-qing, GAO Shu-jun, ZHANG Sui-sheng, GUO Jian-ting, HU Zhuang-qi. The effect of atomic order on environmental embrittlement of an Fe_3Al-based alloy [J]. Mater Lett, 1997, 31(3-6): 227−231.

MA-PAS 和 MA-HP 烧结制备的 Fe_3Al 金属间化合物的组织和力学性能

王 建[1]，邢建东[2]，汤慧萍[1]，杨保军[1]，李亚宁[1]

1. 西北有色金属研究院 金属多孔材料国家重点实验室，西安 710016；
2. 西安交通大学 金属材料强度国家重点实验室，西安 710049

摘 要：以机械合金化 Fe-28%Al(摩尔分数)合金粉末为原料，分别采用等离子活化烧结(PAS)和热压烧结(HP)方法制备致密度高达 99%的 Fe_3Al 金属间化合物。XRD 和 TEM 测试结果表明：PAS 烧结试样保留了机械合金化粉末的 A2 无序结构，并呈现出亚微米晶粒区域(>1 μm)和纳米晶粒区域(<500 nm)双峰分布的特征，而 HP 烧结试样为部分 $D0_3$ 有序结构，晶粒尺寸在 1~2 μm 的范围内。压缩试验表明：在室温至 800 °C 的条件下，采用两种方法烧结的 Fe_3Al 金属间化合物具有近似的压缩强度，虽然当温度超过 400 °C 后压缩屈服强度均急剧下降，但在 800 °C 时其压缩屈服强度仍高达 100 MPa，远高于铸造态 Fe_3Al 金属间化合物。相比于 HP 烧结和铸造态 Fe_3Al 金属间化合物，PAS 烧结 Fe_3Al 金属间化合物表现出优异的室温塑性，其室温压缩工程应变为 20%。组织结构分析和力学性能测试结果表明，超细晶无序组织有利于 Fe_3Al 金属间化合物室温塑性和高温强度的同时增强。

关键词：Fe_3Al 金属间化合物；等离子活化烧结；热压烧结；显微组织；力学性能

(Edited by YANG Hua)